Chapter 5

Paleo-Hydrology

Dream is not what you see in sleep, dream is something which doesn't let you sleep.

- Dr. A.P.J. Abdul Kalam

CHAPTER 5 PALEO-HYDROLOGY

5.1 Introduction

Hydrology is a branch of geoscience that deals with the water; its movement, quality and water cycle. It also broadly deals with water-land-atmosphere interactions, where studies related to modern floods make important part. Paleo-hydrology is a study of past flood records, which accounts the flooding history beyond the instrumental records. Paleofloods in mountains are generated due to extreme rainfall events, cloud bursts, landslide dam lake outburst floods (LLOFs) and glacial lake outburst floods (GLOFs) that occur as a discrete event or climatically modulated series of events (Kale, 2004; Korup et al., 2006; Srivastava et al., 2008; Dobhal et al., 2013; Ziegler et al., 2014; Sundriyal et al., 2015; Srivastava et al., *in communication*). The Himalaya forms the water tower for nearly $1/6^{th}$ of the global population, therefore, long term flood history of the Himalayan Rivers is important to model future water availability and where the records of past floods are rare. The floods, in long run, are important agents that help to build-up the landscape. A big debate on the water availability vis-à-vis fluvial aggradation and incision (Bookhagen et al., 2005; Srivastava et al., 2008; Ray and Srivastava, 2010; Scherler et al., 2015). Therefore, it is important to reconstruct longer flood histories of rivers from different climate domains of the Himalaya. The study related to past flood records and its interrelation with landform of this terrain (Ladakh Himalaya), can lead us to make a better land use planning

and reduce the vulnerabilities from the events such as Leh cloud burst-2010, flood in Shyok and Indus-2015, flash floods in Kedarnath-2013, and Kashmir-2015.

Given the status, paleoflood studies in the Himalaya are sparse, where slack water deposits (SWDs) were utilized to reconstruct floods (Kale, 2004; Srivastava et al., 2008; Wasson et al., 2013; Srivastava et al., *in communication*). Rivers of extra Himalayan regions are rather well studied in this aspect (Kale et al., 1996, 2000, 2003; Kale and Hire, 2004; Sridhar, 2007; Sridhar et al., 2013). The SWDs are the couplets of sand-silt and clay with finning upward sequences deposited in the region of reduced flow during the floods. These reduced flow velocity zones are: (1) irregular channel margin, (2) sharp bend, and (3) back flooded tributaries (Baker, 1987; Kochel and Baker, 1982). In the aggraded valleys, where the sequences are made up of channel bars, the paleo-floods can be estimated using grain geometry by calculating the paleo-discharge using theoretical as well as empirical formulas (Costa, 1983; Dortch et al., 2011; Mears, 1979; O'Connor, 1993; Stokes et al, 2012).

The rivers in Himalaya, carry large clasts and make gravel bars during the floods. Therefore, in the vertical sequence that border these rivers, the gravel size, shape, and imbrication data can be used to estimate past flood hydrology. This estimation will also have bearing on the hydrodynamics of the river leading the valley aggradation. Therefore, paleo-hydrological calculations of Indus River using clast geometry, from chronologically constrained sequences, has been carried out in this work. Both theoretical and empirical technique have been applied to

calculate maximum paleo-discharge of the Indus (Costa, 1983; Dortch et al., 2011; Mears, 1979; O'Connor, 1993).

5.2 Theory of Paleo-Hydrology calculation

In any river, sediment grains start moving, when the overall fluid forces (drag and lift) exceed the gravitational and cohesive forces (Reineck and Singh, 1973). The water flow velocity, grain size and grain texture are the important parameters, which can affect the grain entrainment process and therefore, can be used to decipher flow velocity and discharge. Using this method, a catastrophic floods in Front Range of Colorado in 1976 (Costa, 1983), late Pleistocene Bonneville flood (O'Connor, 1993); paleoflood of the Rio Almanzora, Spain (Stokes et al., 2012), and the Mahi river, western India (Sridhar et al., 2013) were estimated.

5.3 Gravel geometry and Empirical formulae

To minimize the friction introduced by gravel to the riverbed in critical entrainment velocity of the gravel surface, incorporates the longest and the intermediate axis of prolate ellipsoid gravel, align along the flow direction. The long axis lies here perpendicular to the flow direction. This mechanism imbricate the gravels opposite to the flow direction and are transported as bedload. In the field, this, identified as most prominent lithofacies, termed as *clast supported horizontally bedded gravels* (Gh; Fig 5.1 A), which is used as a tool to calculate the incipient velocity for the largest gravel on the riverbed. Minimum ten numbers of sorted boulders has been taken into consideration to evaluate clast geometrical data. The clast data includes longest (D_L), intermediate (D_I) and shortest (D_S) diameters, imbrication angle (Θ)

and litho-type (Fig 5.1 B). The paleo-velocity at the riverbed has been calculated using empirical equation after Costa, 1983 (equation 1 and 2). The present day riverbed clasts data are used in equation 1 to generate a model equation followed by the clasts at the riverbed of the Indus River (equation 5), which is further used to calculate the paleo-riverbed velocity.

$$v_b = \frac{2(\gamma_s - \gamma_f) D_I g \mu}{\gamma_f (C_L - C_D')} \quad (1)$$

$$v_b = 0.18 D_I^{0.49} \quad (2)$$

where, v_b = riverbed velocity, D_I = intermediate diameter of largest clast, γ_c and γ_f = specific weight of clast and water respectively, g = acceleration due to gravity, μ= coefficient of static friction, C_L and C_D'= lifting coefficient and adjusted dragging coefficient. The adjusted dragging coefficient ($C_D' = 75\ \% C_D$) were taken into consideration because when the clast rests on the riverbed, whole area of clast do not participates in dragging (Costa, 1983). The clast in the field were selected so that the shape factor SF= $D_S/\sqrt{D_I D_L}$ remains 0.6. The riverbed flow in the Himalaya rivers, where the slope is high, considered as turbulent flow, therefore the average velocity ($\bar{v}$) is factored by 1.2 to obtain velocity (v_b).

$$\bar{v} = 1.2\ v_b \quad (3)$$

$$Q = A.\ \bar{v} \quad (4)$$

Where Q = paleo-discharge (m^3/sec) and A= valley width × depth (thickness of individual sedimentary unit)

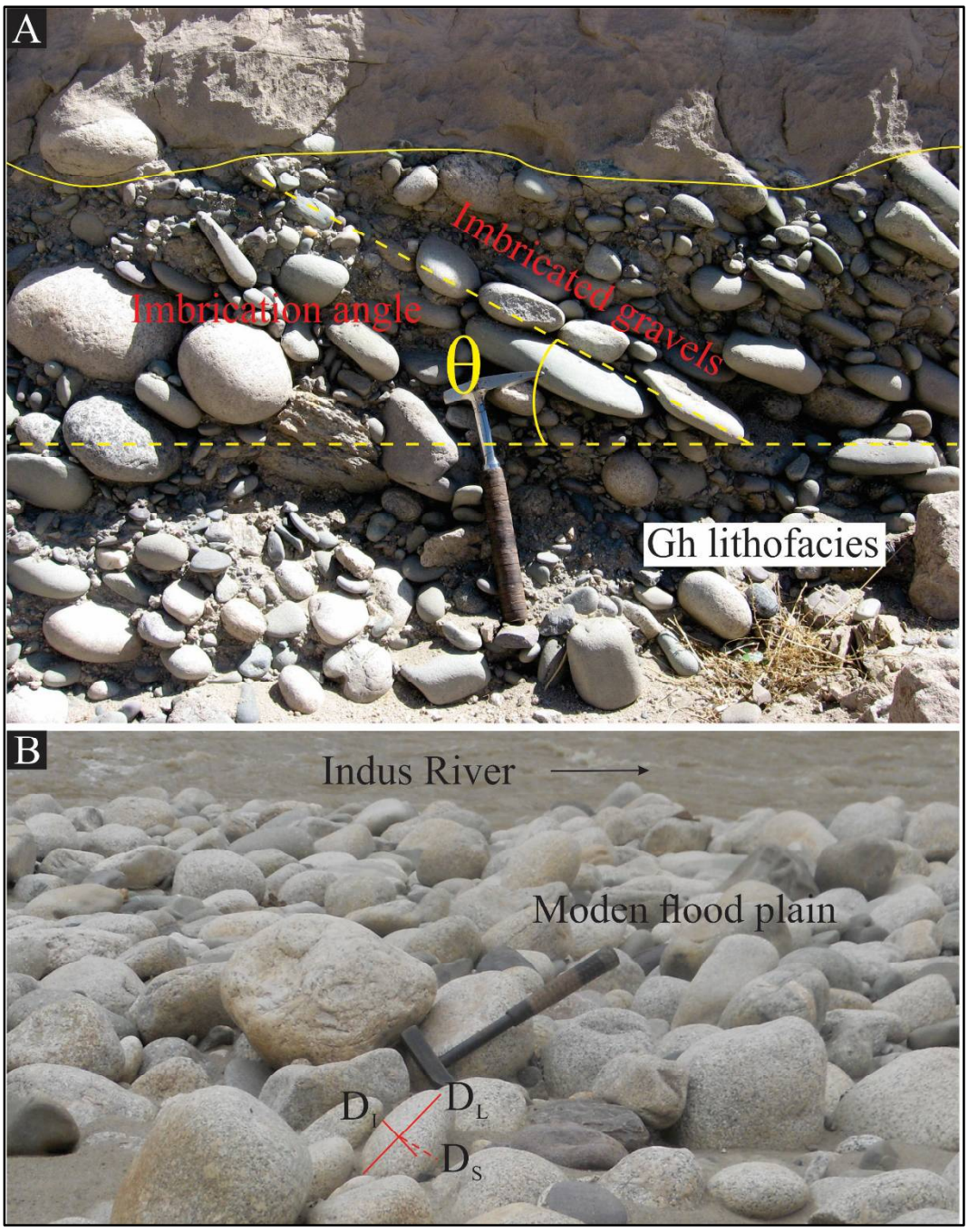

Figure 5.1 (A) Clast supported gravels (Gh facies) showing imbrication angle (θ). (B) Photograph showing clast data: longest (D_L), intermediate (D_I) and shortest (D_S) diameters, imbrication angle (Θ) and litho-type.

The values of lifting (C_L) and dragging (C_D) coefficients were considered as 0.178 and C_D = 1.05 for SF=0.6 (Costa, 1983). The friction between clast and riverbed have inverse relationship with the riverbed velocity. The value for the coefficient of static friction (μ) is considered as 0.7 (Costa, 1983) for this study.

Sections for paleo-discharge estimation

Out of eighteen studied sections, the clast data were collected from eight sections to calculate modern as well as paleo-discharge of the Indus River (Fig 5.2). Five sections: Mahe-R, Kesar, Kiari, Tirido, Hymia-R, Upshi-L, Stakna and Spituk were identified in the field, where clast imbrication data was collected from the modern channel bar and from the vertical sequences (except Upshi). This was done to compare the modern and paleo-discharge.

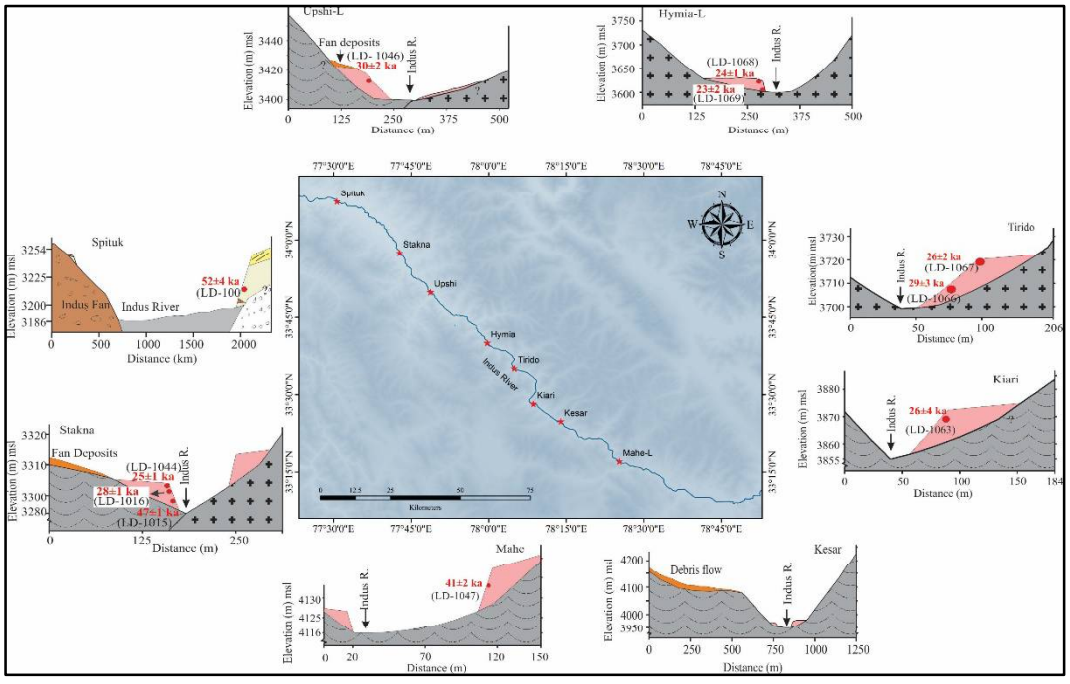

Figure 5.2 Inset map shows the location of sites and their valley cross-sections, where the paleo-discharge was estimated.

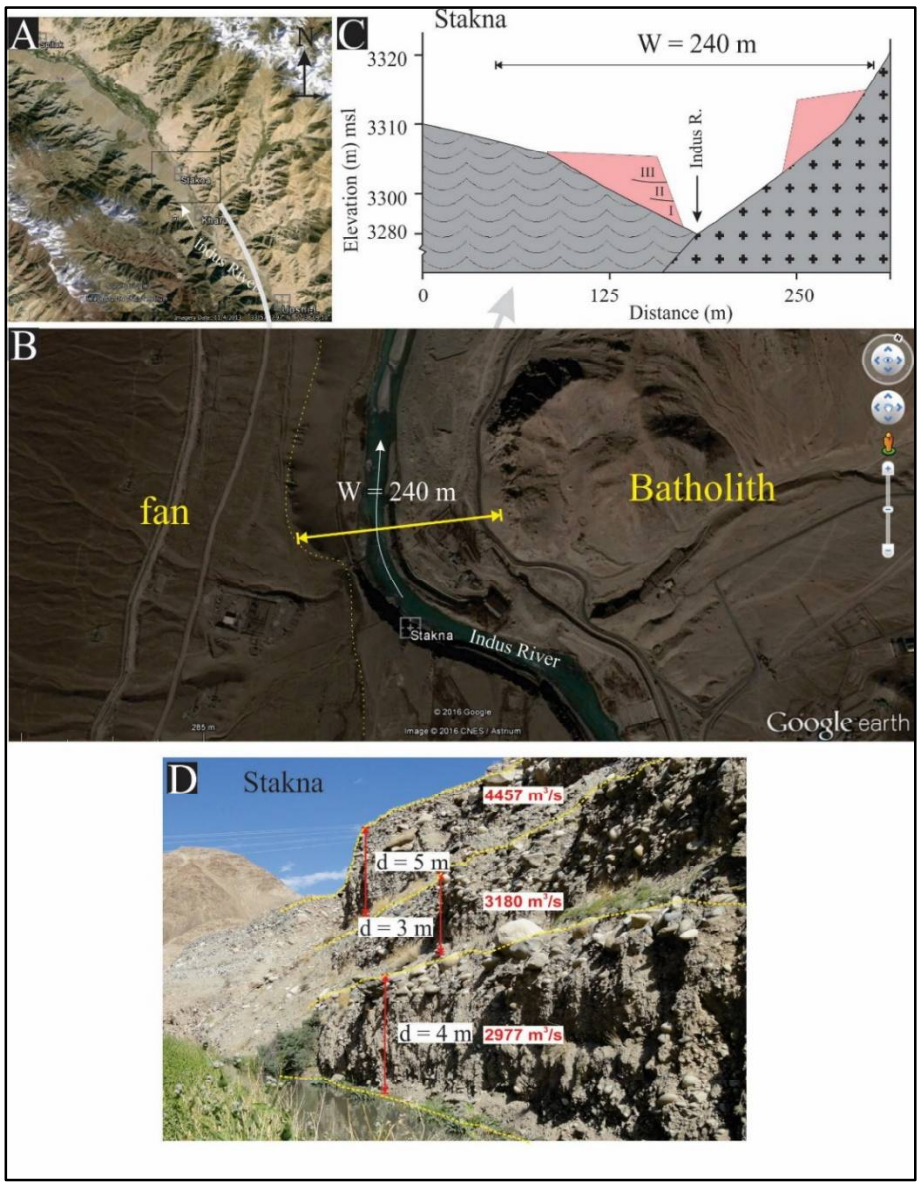

Figure 5.3 (A) Location map of Leh valley. (B) Google image shows Stakna section. From north of the Indus River, fans from batholith and from south, fans from Indus Molasse bound the valley. Here the valley width is measured 240 m. (C) Valley cross-section of Stakna section. (D) A photograph of Stakna section shows individual unit thickness, which represents the individual bar thickness and ultimately river depth (d).

5.4 Discharge calculation

The palaeo-discharge estimation requires calculation of flow velocity and channel cross section at bankfull depth. The measurements of palaeo-channel cross section is difficult and imparts error in the results. Area (A) is calculated by multiplying the valley width with the thickness of the sedimentary unit of which the clast geometry is considered (d; Fig 5.3).

The thickness of the unit can also represent the contemporary river depth or hydraulic radii. As in discussion on the facies (Chapter 4), the Gh facies represent the channel bar aggradation, and treated as bedload, the velocity thus calculated, will represent the riverbed velocity responsible for bar aggradation. DEM of SRTM 90 m is used to estimate valley width and slope of each studied section. The valley width and slope calculations were cross-checked by measurement done on SOI (1:50:000) topographic map. A model equation (equation 5) was generated using the modern riverbed clast geometric and composition data (Fig 5.4).

$$v_b = 0.176 D_I^{0.54} \qquad (5)$$

The equation (2) and (5) has slight difference that is because these are belonging to two different river systems. Both are different in riverbed topography, type of bedload, river cross-section and their annual discharge, which has been to be taken into consideration to generate empirical formulas.

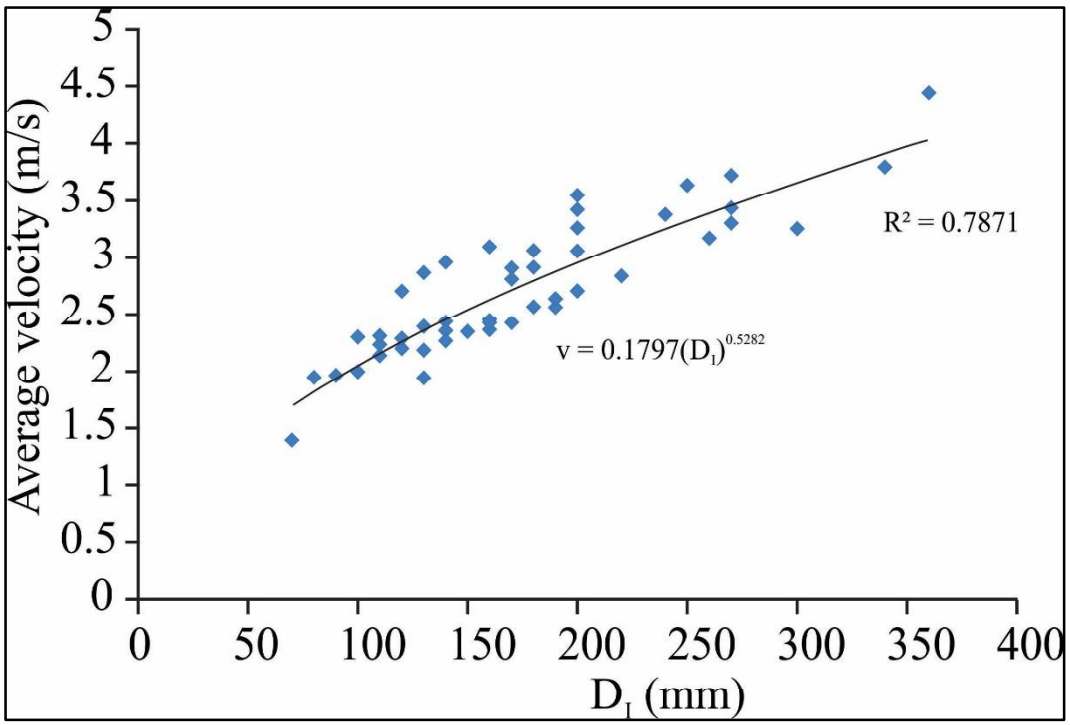

Figure 5.4 A model showing the relation of intermediate clast size with its average velocity. Coefficient of correlation (R^2) is ~ 80 %, which suggest strong correlation.

Table 5.1 Intermediate clast size of modern riverbed clasts (D_I), riverbed velocity, average velocity, average area and modern riverbed discharge of five studied section along the Indus River.

D_I (mm)	**Riverbed velocity, v_b (m/sec) using Costa, 1983**	**Average velocity, $\overline{v}$**	**Av. Area (W×D)**	**Modern riverbed discharge ($m^3 s^{-1}$)**
Mahe-R (4132 m asl)				
70	1.72	2.06	216	445
100	2.08	2.50	216	539
110	2.19	2.63	216	567

100	2.08	2.50	216	539
120	2.29	2.75	216	594
90	1.97	2.36	216	509
140	2.49	2.99	216	646
120	2.29	2.75	216	594
110	2.19	2.63	216	567
130	2.39	2.87	216	620
Kesar (3958 m asl)				
200	3.02	3.62	483	1748
250	3.40	4.08	483	1970
360	4.13	4.96	483	2395
270	3.54	4.25	483	2053
260	3.47	4.16	483	2012
340	4.01	4.81	483	2323
300	3.75	4.50	483	2172
140	2.49	2.99	483	1443
240	3.32	3.99	483	1927
270	3.54	4.25	483	2053
Tirido (3780 m asl)				
270	3.54	4.25	235.8	1002
190	2.93	3.52	235.8	830
140	2.49	2.99	235.8	705
200	3.02	3.62	235.8	853
200	3.02	3.62	235.8	853

170	2.76	3.32	235.8	782
170	2.76	3.32	235.8	782
180	2.85	3.42	235.8	806
160	2.68	3.21	235.8	757
200	3.02	3.62	235.8	853
Upshi-L (3400 m asl)				
130	2.39	2.87	798	2292
170	2.76	3.32	798	2646
190	2.93	3.52	798	2809
160	2.68	3.21	798	2562
140	2.49	2.99	798	2385
130	2.39	2.87	798	2292
110	2.19	2.63	798	2096
120	2.29	2.75	798	2196
180	2.85	3.42	798	2729
80	1.84	2.21	798	1767
Stakna (3280 m asl) Unit-1				
160	2.68	3.21	288	925
220	3.17	3.81	288	1097
180	2.85	3.42	288	985
140	2.49	2.99	288	861
130	2.39	2.87	288	827
200	3.02	3.62	288	1042
150	2.58	3.10	288	893

200	3.02	3.62	288	1042
160	2.68	3.21	288	925
190	2.93	3.52	288	1014

Table 5.2 comprises the paleo-discharge of seven sections studied along the Indus River of Segment II and Segment III. Table 5.1 gives the details including clast geometry data, riverbed velocity (ranging from 1.72 to 4.13 m s^{-1}) calculated using equation 1, average river velocity (2.06 – 4.99 m s^{-1}) calculated using equation 3, average area (A), and modern riverbed discharge (using equation 4). The average area was calculated by multiplying the valley width and modern river depth. District administration records and published data suggest that the occurrence of major floods in the Indus River and its catchment are very common (Juyal, 2010; Hobley et al., 2012; Thayyen et al., 2013). A peak discharge of Indus, as recorded for the month of August (2002-2004 and 2006) at Leh station (Segment III), fluctuated from 130-250 $m^3 s^{-1}$ (Fig 5.5), with 198 ± 45 $m^3 s^{-1}$ as mean (± stdev). However, during extreme events an abrupt increase in discharge was noticed at Alchi Dam, ~ 50 km downstream of the Leh, in August 2006 and August 2010, (1846 $m^3 s^{-1}$ and 1940 $m^3 s^{-1}$ respectively; Srivastava et al., *in communication*). The discharge data generated from gravels of modern riverbed comes near to that observed during extreme events.

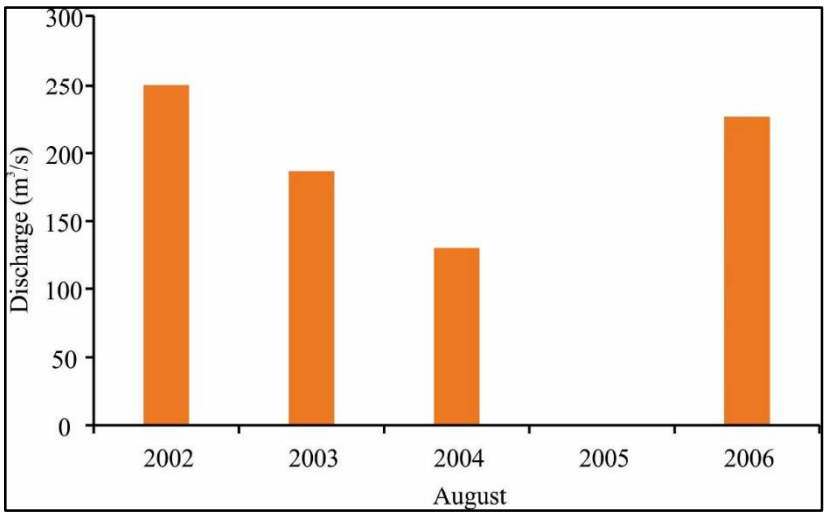

Figure 5.5 Modern discharge of the Indus River from 2002 to 2006, at Leh station.

Table 5.2 Intermediate clast size, riverbed velocity, average velocity, average area and paleo-discharge of the Indus River.

D_I (mm)	**Modelled riverbed velocity, v_b (m/sec)**	**Average velocity, $\overline{v}$**	**Av. Area (W×D)**	**Palaeo-discharge ($m^3 s^{-1}$)**
Mahe (4132 m asl)				
150	2.58	3.10	213.76	663
110	2.19	2.63	213.76	561
150	2.58	3.10	213.76	663
340	4.01	4.81	213.76	**1028**
220	3.17	3.81	213.76	814
220	3.17	3.81	213.76	814
200	3.02	3.62	213.76	773
160	2.68	3.21	213.76	686
140	2.49	2.99	213.76	639
100	2.08	2.50	213.76	533
Kesar (3958 m asl)				
180	2.85	3.42	632.5	2163
320	3.88	4.66	632.5	2945

180	2.85	3.42	632.5	2163
300	3.75	4.50	632.5	2844
140	2.49	2.99	632.5	1890
170	2.76	3.32	632.5	2098
110	2.19	2.63	632.5	1661
290	3.68	4.42	632.5	2793
860	6.59	7.91	632.5	**5003**
270	3.54	4.25	632.5	2688
Kiari (3854 m asl)				
80	1.84	2.21	230.46	510
200	3.02	3.62	230.46	**834**
100	2.08	2.50	230.46	575
80	1.84	2.21	230.46	510
90	1.97	2.36	230.46	543
120	2.29	2.75	230.46	634
100	2.08	2.50	230.46	575
90	1.97	2.36	230.46	543
140	2.49	2.99	230.46	689
200	3.02	3.62	230.46	834
Tirido (3780 m asl)				
160	2.68	3.21	786	2523
80	1.84	2.21	786	1740
120	2.29	2.75	786	2163
120	2.29	2.75	786	2163
140	2.49	2.99	786	2349
80	1.84	2.21	786	1740
140	2.49	2.99	786	2349
210	3.10	3.71	786	2919
240	3.32	3.99	786	**3136**
220	3.17	3.81	786	2993
Hymia-R (3602 m asl)				
160	2.68	3.21	768	2465
140	2.49	2.99	768	2295
240	3.32	3.99	768	**3064**
230	3.25	3.90	768	2995
110	2.19	2.63	768	2017
140	2.49	2.99	768	2295
210	3.10	3.71	768	2853
130	2.39	2.87	768	2206
90	1.97	2.36	768	1811
140	2.49	2.99	768	2295
Stakna (3280 m asl) Unit-1				
90	1.97	2.36	960	2264
50	1.43	1.72	960	1652

80	1.84	2.21	960	2125
90	1.97	2.36	960	2264
150	2.58	3.10	960	**2977**
110	2.19	2.63	960	2521
70	1.72	2.06	960	1978
90	1.97	2.36	960	2264
50	1.43	1.72	960	1652
130	2.39	2.87	960	2757
Unit-2				
200	3.02	3.62	720	2605
160	2.68	3.21	720	2311
290	3.68	4.42	720	**3180**
200	3.02	3.62	720	2605
200	3.02	3.62	720	2605
100	2.08	2.50	720	1796
170	2.76	3.32	720	2388
90	1.97	2.36	720	1698
160	2.68	3.21	720	2311
120	2.29	2.75	720	1981
Unit-3				
210	3.10	3.71	1200	**4457**
120	2.29	2.75	1200	3302
190	2.93	3.52	1200	4224
170	2.76	3.32	1200	3980
160	2.68	3.21	1200	3852
130	2.39	2.87	1200	3446
130	2.39	2.87	1200	3446
150	2.58	3.10	1200	3721
120	2.29	2.75	1200	3302
80	1.84	2.21	1200	2657
Spituk (3181 m asl)				
50	1.43	1.72	1693	2913
80	1.84	2.21	1693	3748
100	2.08	2.50	1693	**4224**
90	1.97	2.36	1693	3992
100	2.08	2.50	1693	4224
90	1.97	2.36	1693	3992
80	1.84	2.21	1693	3748
50	1.43	1.72	1693	2913
40	1.27	1.53	1693	2584
80	1.84	2.21	1693	3748

5.5 Paleo-discharge and past climate

The rivers of southern front of the Himalaya largely receive water from ISM and flood during the monsoon months (JJAS) that is the time when most of the sediment from hill slopes are mobilized into the valleys. The sediment will be aggraded in the channel or flushed out will depend upon the flood discharge. In drier Himalaya such as the Ladakh snowfall, glacial melt, westerlies intensity and the ISM bound rainfall control the discharge. However it has been observed in the paleo records that during the wetter climatic phases the ISM plays a dominant role in shaping hydrology of the region e.g. the records from Tso Kar and Chandra Tal show increased ISM bound precipitation during the Holocene optimum (Wünnemann et al., 2010; Rawat et al., 2015). Likewise, there are instances in the mid Holocene, when the large amount of sediment was mobilized into the channels and large number of landslides were triggered leading to valley aggradation (Bookhagen et al., 2005; Korup et al., 2007; Dortch et al., 2009; Juyal et al., 2010; Ray and Srivastava, 2010; Srivastava et al., 2013). Abnormal monsoon years and climatically wetter phases were believed responsible (Srivastava et al., 2008; Phartiyal et al., 2009). The recent events of cloud bursts and floods in Ladakh also occurred during monsoon months e.g. flood in 2006 was on July 31 and August 1, and in 2010 it was 2 – 4 August (Juyal, 2010; Hobley et al., 2012; Thayyen et al., 2013). This implies that larger floods, valley aggradation and incision are rather controlled by varying strength of the ISM in the region.

There is an ongoing debate on whether the river aggradation occurs during the wet climatic phases when the river has higher competence and carrying capacity

or during the drier climatic conditions when the river has higher sediment to water ratio (Bull, 1991; Pazzaglia et al., 1998; Hancock et al., 1999; Blum and Törnqvist, 2000; Srivastava et al., 2008; Ray and Srivastava, 2010; Scherler et al., 2015). The sequences that are utilized to generate paleo-discharge data, represent the phase of valley aggradation. Therefore, this discharge data provides good proxy record when the river was aggrading and hence bears great significance to the debate.

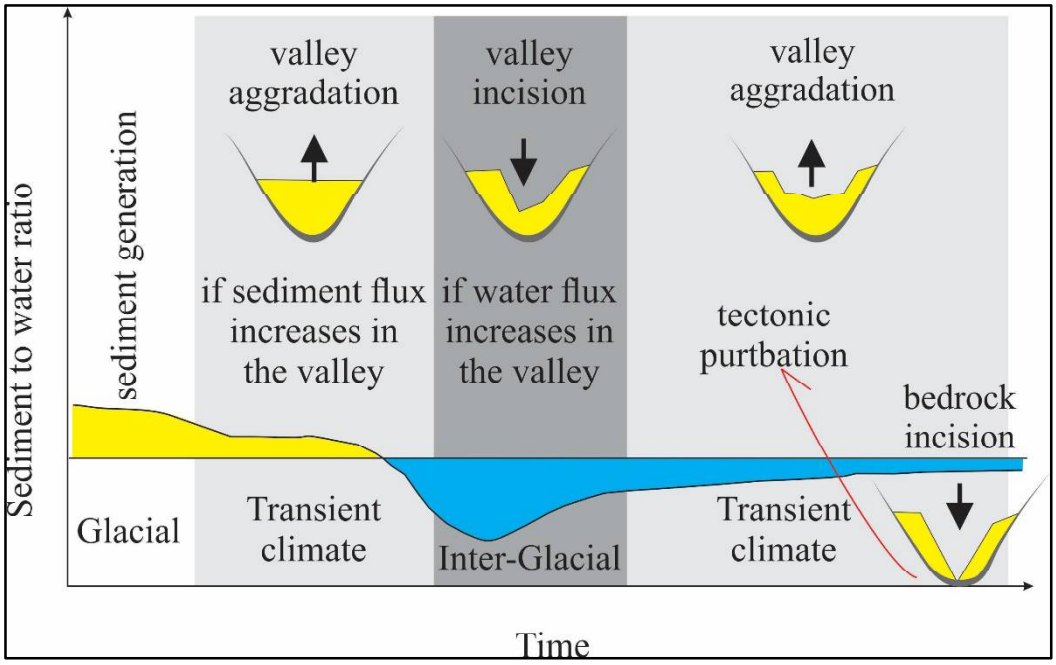

Figure 5.6 A model showing Himalayan river response to glacial to inter-glacial climate change. The aggradation of a Himalayan rivers occurred during transient climate when sediment to water ratio was higher.

Discharge was estimated from the sequence that represent valley aggradation during 47 – 23 ka. The estimated paleo-discharge from Mahe to Spituk along the Indus is varied from 834 to 5003 $m^3 s^{-1}$. As the aggraded sequences develop in relatively higher sediment to water ratio (enhanced sediment supply), hence the paleo-discharge of these section represent the equivalent fluvial condition. The chronology of the sequences suggest that the aggradation occurred during 47 – 23 ka in warm and wet climatic conditions (MIS 3; Prell and Kutzbach, 1987; Jung et al., 2009; Srivastava et al., 2013; Dutt et al., 2015). The geomorphic data from Indus and rivers from all across Himalaya suggest that the major incision phase commenced during the Holocene optimum (14-10 ka; Burbank et al., 1996; Leland et al., 1998; Lavè and Avouac, 2001; Mukul et al., 2007; Srivastava and Misra, 2008; Srivastava et al., 2009, 2013; Ray and Srivastava, 2010; Juyal et al., 2010). The discharge of SWDs of the Indus during incision phase, were dated between 13-9 ka and located at ~100 m upstream to the Indus-Zanskar confluence zone (Srivastava et al., *in communication*). The paleoflood discharge of these SWD sequences are ranging from 30,300 – 40,000 $m^3 s^{-1}$.

Therefore, our data suggests that during aggradation (47–23 ka), the discharge of the Indus was higher by the factor of ten than the modern day discharge, whereas in early Holocene (14 – 10 ka), when the valley incised, it was further ten folds higher. Hence the aggradation in valley occurred during transient climate when sediment to water ratio was higher, however, incision initiated when sediment to water ratio become very less, during post glacial wet climatic phase (Fig 5.6).